Mechanisms of Reaction of Sulfate Esters: A Molecular Orbital Study of Associative Sulfuryl Group Transfer, Intramolecular Migration, and Pseudorotation

Dale R. Cameron† and Gregory R. J. Thatcher*

Department of Chemistry, Queen's University, Kingston, Ontario, K7L 3N6 Canada

Received December 4, 1995⊗

Molecular orbital calculations for the reactions of 2-hydroxyethyl sulfate in neutral and ionized forms were used to examine the free energy profiles for intramolecular sulfuryl group transfer in the gas phase. Detailed analysis of reaction dynamics yielded structures for trigonal bipyramidal pentacoordinate reaction intermediates and for transition states at the MP2/6-31+G*//HF/3-21+G(*) and MP2/6-31+G*//HF/3-21G(*) levels of calculation for anionic and neutral species, respectively. Application of a continuum dielectric model to these structures provided estimated free energy profiles for reaction in aqueous solution. Comparison with the reactivity of phosphate esters suggests that the empirical guidelines for reactions of phosphates may, in large part, be extended to reactions of sulfate esters. It is predicted that the activation barriers to intramolecular sulfuryl group transfer will be large, in accord with experiment and in contrast with phosphoryl transfer. The explanation is based upon (1) the requirement for the energetically unfavorable protonation of the sulfate moiety for nucleophilic attack on sulfur; and (2) the relatively higher energy of the pentacoordinate relative to the tetracoordinate state for S over P species. However, Berry pseudorotation is facile and does not present a barrier to reaction. The calculations suggest that nucleophilic substitution of alkoxide on the protonated sulfate moiety has a low activation barrier and may occur with inversion or retention of stereochemistry at sulfur.

Introduction

Sulfate esters are found in many biomolecules from steroid sulfates and aryl sulfates, such as dopamine sulfate, to sulfurylated carbohydrates.[1] Sulfate monoesters carry a negative charge at physiological pH, and therefore, sulfurylation may be used to drastically increase the hydrophilicity of a lipophilic molecule. Indeed, detoxification through sulfate conjugation by sulfotransferase enzymes represents the most well-understood biological role of sulfate esters.[2] However, in addition to simply increasing water solubility, the specific regiochemical and stereochemical placement of sulfate groups may lead to more subtle and more profound biological effects. The glycosaminoglycan (GAG) sulfates, such as heparin, heparan sulfate, and chondroitin sulfate, are oligosaccharides functionalized regiospecifically with sulfamidate and sulfate ester functionalities.[3] These GAG sulfates form an integral part of many cell surface proteoglycans and it seems clear that in this way GAG sulfates play a major role in cell−cell recognition, aggregation, and motility. Indeed, recently the realization of the importance of the sulfate group in biomolecular recognition has inspired therapeutic strategies directed at mimicking GAG sulfates in treatment of disease states including AIDS and Alzheimer's.[4]

It is useful to draw comparisons between sulfate and phosphate esters. It has been said that phosphate esters dominate the living world.[5] Phosphate diesters include ATP, membrane phospholipids, and the backbone of DNA. Phosphates are used as biological activating groups and perform an essential recognition function in small secondary messenger molecules such as the nucleotide cyclic monophosphates and inositol phosphates. The many and significant biological roles of phosphate mono and diesters are attested to by the large body of work directed at understanding the structure, function, and in particular, reactivity of simple phosphate esters.[6,7] This extensive body of work has allowed Westheimer to formulate a compelling answer to the question: *Why did nature choose phosphates?*[5] In comparison, study of the structure and reactivity of simple sulfate esters, in particular alkyl sulfate monoesters has attracted less attention.[8,9] No attempt has been made to answer the complementary question: *Why did nature choose sulfates?*

Clearly, the biological roles of the superficially similar sulfate and phosphate esters are very different. What features of the reactivity of simple sulfate esters makes them suitable for a leading role in biomolecular recognition, but unsuitable for the various biological roles associated with phosphate esters? In order to address this question we have completed a series of molecular orbital (MO) calculations directed at sulfate esters and the reactive intermediates involved in sulfate group transfer. As far as we are aware this is the first *ab initio*

† Current address: BioMega (Boehringer Ingelheim) Research Inc., 2100 Cunard St., Laval, QU H7S 2G5, Canada.

⊗ Abstract published in *Advance ACS Abstracts,* July 15, 1996.

(1) Huxtable, R. J. *Biochemistry of Sulfur*; Plenum Press: New York, 1986.

(2) Williams, D. A. In *Principles of Medicinal Chemistry,* 3rd ed.; Foye, W. O., Ed.; Lea and Febiger: Philadelphia, 1990.

(3) Jackson, R. J.; Busch, S. J.; Cardin, A. D. *Physiol. Rev.* **1991**, *71*, 481.

(4) Kisilevsky, R.; Lemieux, L. J.; Fraser, P. E.; Kong, X.; Hultin, P. G.; Szarek, W. A. *Nature Med.* **1995**, *1*, 143. Moriya, T.; Kurita, H.; Matsumoto, K.; Otake, T.; Mori, H.; Morimoto, M.; Ueba, N.; Kunita, N. *J. Med. Chem.* **1991**, *34*, 2301.

(5) Westheimer, F. H. *Science* **1987**, *235*, 1173.

(6) Thatcher, G. R. J.; Kluger, R. *Adv. Phys. Org. Chem.* **1989**, *25*, 99 and references therein.

(7) Westheimer, F. H. *Acc. Chem. Res.* **1968**, *1*, 70.

(8) Williams, A.; Douglas, K. T. *Chem.* Rev. **1975**, *75*, 627 and references therein.

(9) Williams, A. *Acc. Chem. Res.* **1989**, *22*, 387 and references therein.

S0022-3263(95)02146-3 CCC: $12.00

Table 1. Relative Energy, Solvation Energy, Entropy, Enthalpy, and Free Energy for Anionic Species (kcal/mol)

parameter	**AS**	**BS**	**ATS**$_{endo}$	**AI**$_{TBP}$	**ATS**$_{eq}$	**ATS**$_{exo}$	**cS** + OH^-
rel energy[a]	0.00	68.36	66.86	56.36	61.04	90.78	96.29
rel aq solv energy CHELP[b]	0.00	−14.27	−8.77	−8.83	−2.41	−21.11	−40.58
rel aq solv energy MK1[c]	0.00	−23.34	−9.62	−9.20	−5.59	−27.39	−42.00
rel aq solv energy MK2[d]	0.00	−31.21	−16.18	−13.13	−8.82	−26.96	−42.00
Δh[e]	64.89	62.46	65.31	64.02	63.65	62.33	61.23
rel enthalpy[f]	0.00	63.01	62.03	55.77	59.24	88.22	95.29
S_{tot} (cal mol^{-1} K^{-1})	86.96	95.13	85.13	83.22	81.11	87.34	121.22
E_{zp} (scaled)	54.22	51.30	51.97	53.63	53.66	51.73	50.49
−freq (scaled), cm^{-1}	−	−	−105	−	−243	−104	−
energy + E_{zp} (rel)	0.00	65.44	64.61	55.77	60.48	88.29	92.56
relative free energy	0.00	60.0	62.6	56.0	61.0	85.6	85.1
ΔG + MK2 solv free energy	0.00	28.8	46.4	42.9	52.2	58.6	42.7

[a] MP2/6-31+G*//HF/3-21+G(*), E(**AS**) = −851.7983004 au. [b] CHELP/HF/3-21+G(*) charges. [c] Mulliken/MP2/6-31+G* charges. [d] Mulliken charges; H(O) radius 0.73 Å, $\Delta G_s(OH^-)$ = −98 kcal/mol, ΔG_s(MK2/**AS**) = −71.70 kcal/mol. [e] $\Delta h = E_{trans} + E_{rot} + E_{vib}$. [f] H(rel) = $\Delta E_{MP2} + \Delta h + P\Delta V$ ($P\Delta V = RT$).

Table 2. Relative Energy, Solvation Energy, Entropy, Enthalpy, and Free Energy for Neutral Species (kcal/mol)

parameter	**NS**	**TS**$_{endo}$	**I**$_{endo}$	**TS**$_{PR}$	**TS**$_{rot}$	**I**$_{exo}$	**TS**$_{exo}$[g]	**cS** + H_2O
rel energy[a]	0.00	48.27	36.04	37.99	48.05	35.73	50.84	7.17
rel aq solv energy CHELP[b]	0.00	0.95	−2.26	0.10	−2.63	−0.77	−14.75	−10.46
rel aq solv energy MK1[c]	0.00	−0.23	−0.24	+0.02	−3.31	+0.72	+1.17	−6.86
rel aq solv energy MK2[d]	0.00	+0.62	−5.25	−3.85	−10.21	−1.21	+6.15	−6.86
Δh[e]	73.47	70.67	73.83	73.40	72.36	73.47	69.97	70.56
S_{tot} (cal mol^{-1} K^{-1})	89.58	84.08	83.59	82.60	83.11	89.58	83.19	123.73
rel enthalpy[f]	0.00	43.53	37.33	38.81	48.40	35.40	48.17	−0.29
E_{zp} (scaled)	61.52	59.57	62.45	62.41	61.20	62.53	59.00	63.83
-freq, cm^{-1} (scaled)	−	−684	−	−82	−517	−	−1243	−
energy + E_{zp} (rel)	0.00	46.32	38.79	40.48	51.20	39.77	48.32	20.52
relative free energy	0.00	45.2	38.8	40.6	48.2	33.3	50.1	7.2
ΔG + MK2 solv free energy	0.00	45.8	33.6	36.7	38.0	32.1	56.3	0.3

[a] MP2/6-31+G*//HF/3-21+G(*), E(**NS**) = −852.2755958 au. [b] CHELP/HF/3-21G(*) charges. [c] Mulliken/MP2/6-31+G* charges. [d] Mulliken charges, H(O) radius 0.73 Å, $\Delta G_s(H_2O)$ = −14.26 kcal/mol, ΔG_s(MK2/**NS**) = −30.95 kcal/mol. [e] $h = E_{trans} + E_{rot} + E_{vib}$. [f] H(rel) = $\Delta E_{MP2} + \Delta h + P\Delta V$ ($P\Delta V = RT$). [g] Geometry HF/3-21+G(*).

Scheme 1

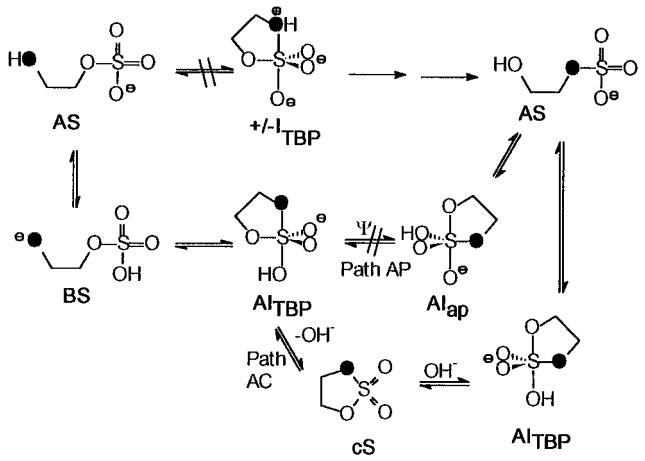

Scheme 2

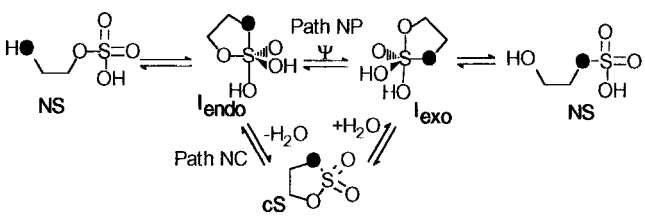

study directed at the pentacoordinate intermediates and transition states involved in the reactions of sulfate esters. The reaction under study is intramolecular sulfuryl group transfer. On the basis of the dogma of mechanistic phosphorus chemistry, pathways may be drawn for intramolecular sulfuryl group transfer from the anionic sulfate reactant **AS** (Scheme 1) and nonionized, neutral sulfate reactant **NS** (Scheme 2). However, there is no unambiguous evidence that the trigonal bipyramidal (TBP) intermediates, Berry pseudorotations, and other mechanistic features of phosphorus chemistry may be applied to nucleophilic substitution at sulfur in sulfate esters.

Methodology

All structures were optimized using the Gaussian 92 program[10] on either an IBM RISC-6000/320e or a RISC-6000/355, using the 3-21+G(*) or 3-21G(*) basis sets.[11] Reaction energy profiles were examined by partial optimizations obtained by freezing the desired (reaction) coordinate at various positions followed by full optimizations near local minima (profile minima). Transition-state optimizations were performed near saddle points (profile maxima).[12] Reaction profiles were thoroughly examined by considering various reaction trajectories.[13] All stationary points were subjected to a normal-mode analysis, and charges were calculated using the Mulliken and CHELP formalisms.[14] Free energies of activation and reaction were determined at 298 K from the thermochemical data found by normal mode analysis (Tables 1 and 2).[12] Energies were corrected for zero point

(10) Frisch, M. J.; Trucks, G. W.; Head-Gordon, M.; Gill, P. M. W.; Wong, M. W.; Forseman, J. B.; Johnson, B. G.; Schlegel, H. B.; Robb, M. A.; Replogle, E. S.; Gomperts, R.; Andres, J. L.; Raghavachari, K.; Binkley, J. S.; Gonzalez, C.; Martin, R. L.; Fox, D. J.; Defrees, D. J. *Gaussian 92 Rev. C*; Gaussian Inc.: Pittsburgh, PA, 1992.

(11) Binkley, J. S.; Pople, J. A.; Hehre, W. J. *J. Am. Chem. Soc.* **1980**, *102*, 939. Clark, T.; Chandrasekhar, J.; Spitznagel, G. W.; Schleyer, P. *J. Comput. Chem.* **1983**, *4*, 294.

(12) Hehre, W. J.; Radom, L.; Schleyer, P. Pople, J. A. *Ab Initio Molecular Orbital Theory*; John Wiley & Sons: Toronto, 1986.

(13) Cameron, D. R. PhD Thesis, Queen's University, 1994.

(14) Chirlian, L. E.; Francl, M. M. *J. Comput. Chem.* **1987**, *8*, 894.

Table 3. Bond Lengths (Å) and Angles for Anionic Sulfuranes and cS[a]

parameter	**AS**	**BS**	**ATS**$_{endo}$	**AI**$_{TBP}$	**ATS**$_{eq}$	**ATS**$_{exo}$	**cS**
∠O1−S−O3 (endo)	62.2	−	75.1	84.2	78.8	90.4	94.7
∠O6−S−O7	115.7	118.0	125.4	127.3	117.5	136.9	120.7
∠O8−S−O1	103.4	−	168.5	167.7	143.7	147.8	−
∠O8−S−O3	−	99.6	93.4	84.3	74.9	63.1	−
∠C4−O3−S	−	126.6	125.1	119.7	115.9	109.2	114.0
∠C5−O1−S	121.5	−	104.2	111.5	117.1	110.4	114.0
d(S−O1)	1.614	4.502	2.47	1.797	1.678	1.638	1.586
d(S−O3)	3.565	1.507	1.565	1.664	1.979	1.569	1.586
d(S−O6)	1.457	1.431	1.440	1.477	1.462	1.426	1.424
d(S−O7)	1.447	1.440	1.431	1.459	1.463	1.327	1.424
d(S−O8)	1.471	1.601	1.632	1.695	1.642	2.907	−
d(O3−C4)	−	1.550	1.491	1.453	1.412	1.462	1.479
d(O1−C5)	1.463	1.389	1.400	1.423	1.438	1.471	1.479

[a] HF/3-21+G(*) geometries. For numbering see structures in text.

Table 4. Bond Lengths (Å) and Angles for Neutral Species and cS[a]

Parameter	**NS**	**TS**$_{endo}$	**I**$_{endo}$	**TS**$_{PR}$	**TS**$_{rot}$	**I**$_{exo}$	**TS**$_{exo}$	**cS**
∠O1−S−O3(endo)	57.7	82.2	86.3	85.4	87.9	86.3	92.1	95.1
∠O6−S−O7	119.9	122.9	120.9	110.5	124.1	120.9	124.4	121.3
∠O8−S−O1	138.5	165.2	160.6	144.3	168.4	160.6	166.1	−
∠O8−S−O3	99.9	94.4	87.1	84.0	83.0	87.1	83.6	−
∠C4−O3−S	121.4	125.3	118.6	115.8	119.1	118.6	116.0	113.8
∠C5−O1−S	65.2	111.0	111.9	115.8	113.8	111.9	113.1	113.8
d(S−O1)	3.385	2.098	1.709	1.665	1.687	1.709	1.618	1.580
d(S−O3)	1.545	1.545	1.612	1.664	1.591	1.612	1.583	1.580
d(S−O6)	1.430	1.527	1.576	1.596	1.635	1.576	1.534	1.415
d(S−O7)	1.4115	1.423	1.436	1.432	1.442	1.436	1.432	1.415
d(S−O8)	1.553	1.579	1.609	1.596	1.592	1.609	1.986	−
d(O3−C4)	1.495	1.489	1.462	1.437	1.467	1.462	1.487	1.470
d(O1−C5)	1.428	1.406	1.429	1.437	1.433	1.429	1.460	1.470

[a] HF/3-21G(*) geometries except **TS**$_{exo}$ HF/3-21+G(*). For numbering see structures in text.

vibrational energy.[12] All imaginary frequencies and zero point energy corrections were scaled by 0.9.[12] Normal-mode analysis was performed on transition-state structures, using Spartan 3.0 running on a Silicon Graphics IRIS INDIGO system, to visualize and confirm that the imaginary frequencies calculated corresponded to the reaction coordinate of interest.[15] Structures corresponding to all stationary points, local and global energy minima, and transition states were subject to point calculations at the MP2/6-31+G* level. Further treatment of these structures with a continuum dielectric solvation model (CDM), as formulated by Lim and Chan, provided free energies of solvation.[16,17] A variety of atomic radii and charges at atoms were input into this CDM model providing different estimates of solvation energy. Arguments have been made about the suitability of the 6-31G* and 3-21(+)G* basis sets for calculations on related tetra- and pentacoordinate phosphorus species and indeed both basis sets have been employed providing a good foundation for comparison.[17−25] In our broad experience with calculations on these systems, results from the two sets are comparable. In the following text, energies refer to calculations at the MP2/6-31+G*//HF/3-21+G(*) and MP2/6-31+G*//HF/3-21G(*) level for anionic and neutral molecules respectively. MP2 free energies and enthalpies are obtained from combining MP2 electronic energies with data from HF normal mode analysis (Tables 1 and 2). In the atom numbering scheme employed, O8, O1, and O3 are the hydroxyl, bivalent apical (or pseudoapical), and bivalent equatorial (or pseudoequatorial) oxygens, respectively (Tables 3 and 4).

Results

Anion Pathways. Pathways for intramolecular sulfate group migration from the ionized, anionic sulfate reactant, **AS**, were examined at the MP2/6-31+G*//HF/3-21+G(*) level (Table 1). Cyclization of hydroxyethyl sulfate (**AS**) may be drawn as leading to the pentacoordinate intermediate (±**I**$_{TBP}$) (Scheme 1). However, an equilibrium structure corresponding to ±**I**$_{TBP}$ could not be located. Indeed, when investigating analogous model sulfurane species ($H_2SO_5^{2-}$), no intermediates with an oxyanion in an apical position could be located as stable stationary points.[25] The alternative route, via cyclization of the tautomer (**BS**), may lead to an alternative pentacoordinate intermediate (**AI**$_{TBP}$). This is an essential step in both speculative mechanisms: (1) the anion−pseudorotational pathway AP and (2) the anion-cyclic sulfate pathway AC (Scheme 1).

Structures were located for **AS** and its tautomer **BS** (Table 3). Upon proton transfer, the large intramolecular hydrogen-bond (H-bond) stabilization (between the hydroxyl and the sulfate group) is lost and the ethylene group rotates to move the oxyanion away from the sulfate group (Figure 1a). The difference in energy between the

(15) Spartan v 3.0, Wavefunction Inc., 18401 Von Karman #210, Irvine, CA 92715.
(16) Chan, S. L.; Lim, C. *J. Phys. Chem.* **1994**, *98*, 692.
(17) Tole, P.; Lim, C. *J. Phys. Chem.* **1993**, *97*, 6212.
(18) Lim, C.; Tole, P. *J. Am. Chem. Soc.* **1992**, *114*, 7245.
(19) Thatcher, G. R. J.; Krol, E. S.; Cameron, D. R. *J. Chem. Soc., Perkin Trans. 2* **1994**, 683. Thatcher, G. R. J.; Campbell, A. S. *J. Org. Chem.* **1993**, *53*, 2272.
(20) Lim, C.; Tole, P. *J. Chem. Phys.* **1992**, *96*, 5217.
(21) Taira, K.; Uebayasi, M.; Maeda, H.; Furukawa, K. *Protein Eng.* **1990**, *3*, 691.
(22) Dejaegere, A.; Karplus, M. *J. Am. Chem. Soc.* **1993**, *115*, 5316. Dejaegere, A.; Lim, C.; Karplus, M. *J. Am. Chem. Soc.* **1991**, *113*, 4353.
(23) Tole, P.; Lim, C. *J. Am. Chem. Soc.* **1994**, *116*, 3922.
(24) Wang, P.; Zhang, Y.; Glaser, R.; Reed, A. E.; Schleyer, P.; Streitweiser, A. *J. Am. Chem. Soc.* **1991**, *113*, 55.
(25) Cameron, D. R. In *ACS Symposium Series*; G. R. J. Thatcher, Ed.; American Chemical Society: Washington DC, 1993; Vol. 539.

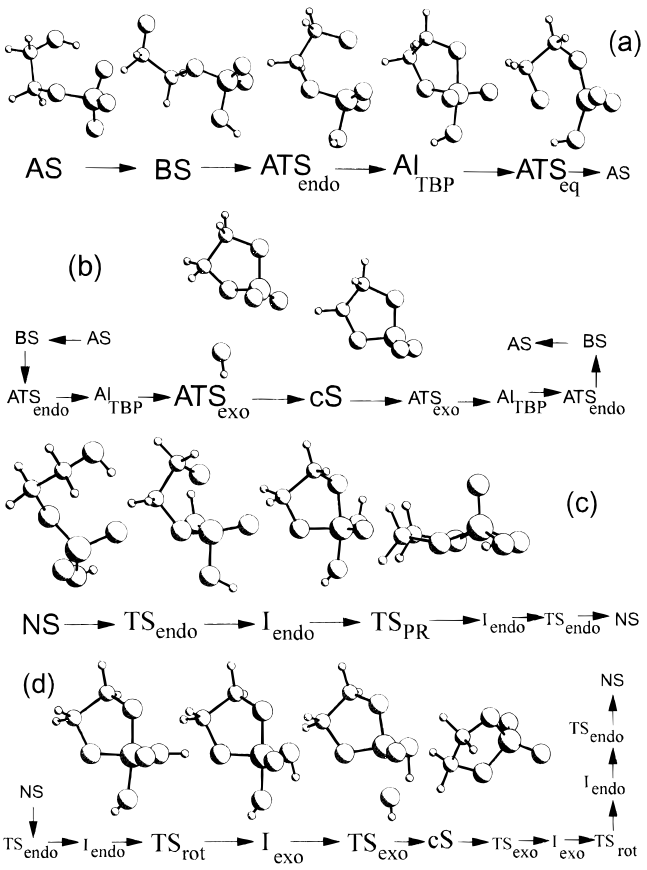

Figure 1. Structures obtained from geometry optimization at HF/3-21+G(*) (a,b) or HF/3-21G(*) (c,d). Only structures in large type are shown for each pathway: (a) pathway CP; (b) pathway AC; (c) pathway NP; (d) pathway NC. See Tables 3 and 4 for geometrical parameters.

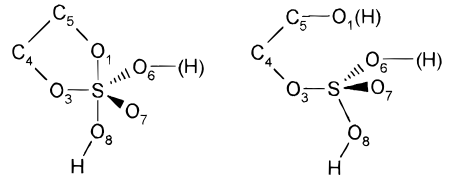

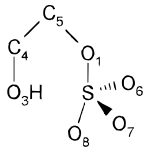

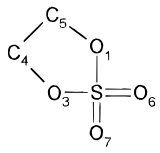

two anionic reactants, **AS** and **BS**, is large (ΔE = 68.4 kcal/mol, ΔG = 66.7 kcal/mol) and in favor of the sulfate anion **AS** (Table 1). Clearly, proton transfer from the hydroxyl to the sulfate group is thermodynamically unfavorable as expected from pK_a values.

Following formation of **BS**, the second step in pathways AP and AC is cyclization, presumably to yield some form of pentacoordinate structure, possibly $\mathbf{AI}_{TBP}$ (Scheme 1). Various approaches of the oxyanion on the sulfur of **BS** were thoroughly examined. The lowest energy approach of the oxyanion proceeds opposite to the S−OH bond and a pentacoordinate transition state is located with the newly forming S−O apical bond length at 2.47 Å. Reaction proceeds as predicted to the TBP intermediate $\mathbf{AI}_{TBP}$. Full structures for $\mathbf{AI}_{TBP}$ and the progenitor transition state $\mathbf{ATS}_{endo}$ are shown in Figure 1a (Table 3). HF energies indicate that the kinetic barrier to ring closure is quite small (2.41 kcal/mol) and the barrier to the reverse ring cleavage reaction is higher, but is also low at 6.61 kcal/mol. There is a large decrease in entropy upon forming the ring-closure transition state, $\mathbf{ATS}_{endo}$, which leads to an increase in the barrier to cyclization. Interestingly, MP2 energies with E_{zp} included, for cyclization of **BS** to give $\mathbf{AI}_{TBP}$ via $\mathbf{ATS}_{endo}$, suggest a spontaneous process (Table 1, Figure 2). Any barrier to cyclization is likely to result from the contribution of $\Delta S^{\neq}$.

Two hypothetical routes exist for intramolecular sulfate transfer from $\mathbf{AI}_{TBP}$: (1) pseudorotation (AP pathway; represented as disallowed in Scheme 1); and (2) exocyclic cleavage to form a cyclic sulfate (AC pathway; Scheme 1). Pseudorotational mechanisms may be examined by progressively altering one of the bond angles along the pseudorotational reaction coordinate and allowing the remainder of the structure to relax.[26,27] The Berry pseudorotation coordinate discussed here is the apical/apical (OSO) bond angle which contracts as pseudorotation progresses. However, other coordinates were examined including the equatorial OSO bond angle and the apical/equatorial angles; all leading to similar results. The distorted TBP structure of $\mathbf{AI}_{TBP}$, with an apical (OSO) angle of 167.7° (TBP ideal ∠ = 180°), was allowed to pseudorotate along the Berry coordinate yielding a transition state ($\mathbf{ATS}_{eq}$) at ∠OSO = 143.7° (Figures 1a and 2).

There are two significant features of this transition state. First, it leads directly to the ring-opened sulfate product **AS** and not $\mathbf{AI}_{TBP}$ (Scheme 1; Figures 1a and 2). Second, S−O bond length changes are not compatible with a simple pseudorotational transition state (Table 3). The pseudoapical and pseudoequatorial S−O bond lengths would have similar values in the idealized square pyramidal (SP), pseudorotational transition state. However, in $\mathbf{ATS}_{eq}$ the pseudoapical bond length has decreased to 1.678 Å from 1.797 Å and the pseudoequatorial S−O bond length has increased to 1.979 Å from 1.664 Å. Clearly this is a transition state for cleavage of the endocyclic, pseudoequatorial S−O bond and not pseudorotation. Furthermore, endocyclic S−O bond breaking in the transition state, $\mathbf{ATS}_{eq}$, is concerted with and assisted by intramolecular proton transfer from the pseudoapical hydroxy to the pseudoequatorial oxygen ligand (Figures 1a and 2).

The transformation of intermediate $\mathbf{AI}_{TBP}$ to the acyclic sulfate product, **AS**, via $\mathbf{ATS}_{eq}$, is an unforeseen pathway for intramolecular sulfate group transfer that does not require a full pseudorotation, nor cyclic sulfate, **cS**, as an intermediate. This may be termed a concerted-pseudorotation (CP) pathway (Figures 1a and 2), since motion along the Berry coordinate is intercepted by concerted intramolecular proton transfer leading to ring cleavage. Furthermore, the calculated energy barrier and the free energy of activation for this ring-opening step ($\Delta G^{\neq}$ = 5 kcal/mol) are low (Table 1; Figure 3). The AC pathway leading to the cyclic sulfate, **cS** + OH^-, requires exocyclic cleavage from $\mathbf{AI}_{TBP}$. The long-range transition state for this process, $\mathbf{ATS}_{exo}$, was found at an S−O bond length of 2.91 Å (Figure 1b). The scissile bond

(26) (a) Wasada, H.; Hirao, K. *J. Am. Chem. Soc.* **1992**, *114*, 16. (b) Cramer, C. J. *J. Am. Chem. Soc.* **1990**, *112*, 7965.
(27) Berry, R. S. *J. Chem. Phys.* **1960**, *32*, 933.

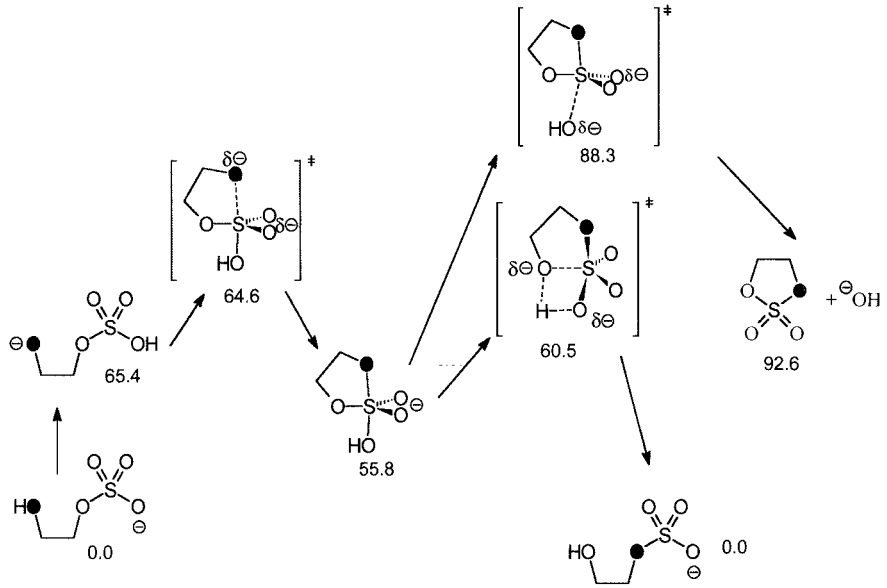

Figure 2. Structures along reaction−energy profile for intramolecular sulfuryl group transer via pathways CP and AC. See Figure 1a,b for detailed structures. Annotated numbers are relative energies including zero point energy, kcal/mol (Table 1). Solid symbols for oxygen atoms are employed in this and other diagrams to better illustrate sulfate migration.

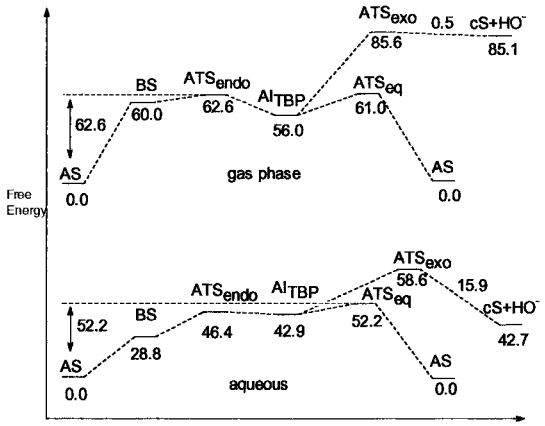

Figure 3. Free energy−reaction profile for pathways CP and AC (see Figures 1 and 2). Numbers shown are relative Gibbs free energies calculated at the MP2/6-31+G*//HF/3-21+G(*) level in the gas phase, kcal/mol. Relative free energies in aqueous solution include a solvation free energy calculated for the gas phase structures (Table 1).

length for the corresponding endocyclic transition state, $\mathbf{ATS}_{endo}$ is considerably shorter (2.47 Å) (Table 3). Owing to the gross destabilization of free hydroxide in the gas phase, the energy profile for exocyclic cleavage suggests that hydroxide plus cyclic sulfate, at infinite separation, is slightly higher in energy than the transition state (Figure 2). However, upon consideration of the free energies, the final products drop in energy due to the large increase in entropy upon dissociation (Table 1, Figure 3). The free energy of activation for exocyclic cleavage from $\mathbf{AI}_{TBP}$ via $\mathbf{ATS}_{exo}$ is approximately 30 kcal/mol. This step represents the rate-determining step for pathway AC in the gas phase: $\Delta G^{\neq}$ for cyclization of **AS** is 86 kcal/mol via this pathway (Table 1, Figure 3). For sulfuryl transfer to occur by pathway AC, the series of steps would be repeated in the reverse direction, from **cS** (eq 1; also see Figure 1b):

$$\mathbf{AS} \rightarrow \mathbf{BS} \rightarrow \mathbf{ATS}_{endo} \rightarrow \mathbf{AI}_{TBP} \rightarrow \mathbf{ATS}_{exo} \rightarrow \mathbf{cS} + OH^- \rightarrow \mathbf{ATS}_{exo} \rightarrow \mathbf{AI}_{TBP} \rightarrow \mathbf{ATS}_{endo} \rightarrow \mathbf{BS} \rightarrow \mathbf{AS} \quad (1)$$

Neutral Pathways. Pathways for intramolecular sulfate group migration may be drawn for the nonionized sulfate ester, **NS**, as reactant. The neutral species were thoroughly examined, at the MP2/6-31+G*//HF/3-21G(*) level, along the two hypothetical pathways: (1) pseudorotational (NP); and (2) via cyclic sulfate (NC) (Scheme 2). Ring closure by apical approach of the alcohol nucleophile on S in **NS** and concerted proton transfer leads to intermediate $\mathbf{I}_{endo}$, which hypothetically may undergo pseudorotation (pathway NP), or exocyclic cleavage to **cS** (pathway NC).

The sulfuryl group of **NS** is tetrahedral and the alcohol oxygen is 3.385 Å from the sulfur atom in the gas-phase equilibrium structure. As the alcohol oxygen approaches sulfur, concerted proton transfer occurs and a transition state was located, with proton transfer more advanced than S−O bond formation at an S−O distance of 2.098 Å. The TBP structure, distorted in $\mathbf{TS}_{endo}$, becomes more evident in the intermediate, $\mathbf{I}_{endo}$, located with an S−O bond length of 1.709 Å (Figure 1c, Table 4). The TBP structure of $\mathbf{I}_{endo}$ is slightly more distorted than that of the monoanionic $\mathbf{AI}_{TBP}$; the apical angle, a measure of this distortion, is 160.6° in the neutral species while it increases to 167.7° in the monoanionic species (Tables 3 and 4; Figure 1a,c). Calculations yield a high activation energy of 46 kcal/mol, but the energy barrier for the reverse ring opening from $\mathbf{I}_{endo}$ is low at 7.5 kcal/mol (Table 2, Figures 4 and 5).

In order to examine the pseudorotation of $\mathbf{I}_{endo}$, the apical O−S−O bond angle was chosen as the reaction coordinate (*vide supra*). In the intermediate $\mathbf{I}_{endo}$ the apical O−S−O bond angle is 160.6° and the equatorial O−S−O bond angle is 124.9°. The transition state for pseudorotation, $\mathbf{TS}_{PR}$, is located with a distorted square pyramidal structure where the *trans*-basal angles are both 144° (Figure 1c, Table 4). The energy of this transition state is only 1.7 kcal/mol above that of $\mathbf{I}_{endo}$ (Figure 4). The free energy of activation for pseudorotation is similarly calculated as a mere 1.5 kcal/mol (Figure 5, Table 2). This indicates a very rapid equilibrium for the isomerization of $\mathbf{I}_{endo}$ and an energetically highly accessible pseudorotational process. Nevertheless,

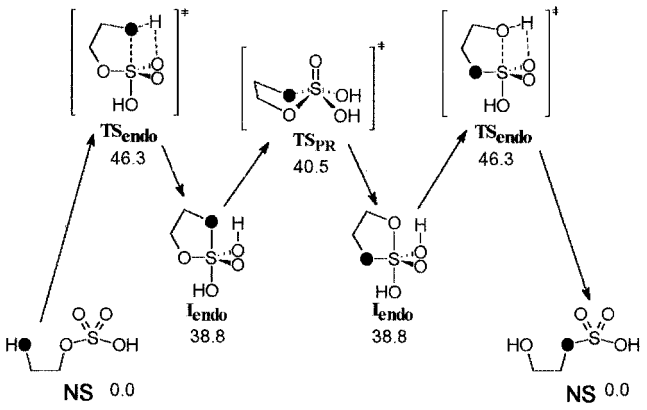

Figure 4. Structures along reaction−energy profile for intramolecular sulfuryl group transfer via pathways NP and NC. See Figure 1c,d for detailed structures. Annotated numbers are relative energies including zero point energy, kcal/mol (Table 2).

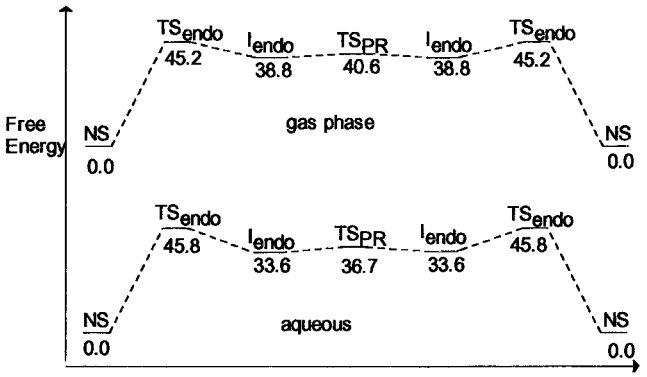

Figure 5. Free energy−reaction profile for pathway NP (see Figures 1 and 4). Numbers shown are relative Gibbs free energies calculated at the MP2/6-31+G*//HF/3-21G(*) level in the gas phase, kcal/mol. Relative free energies in aqueous solution include a solvation free energy calculated for the gas-phase structures (Table 2).

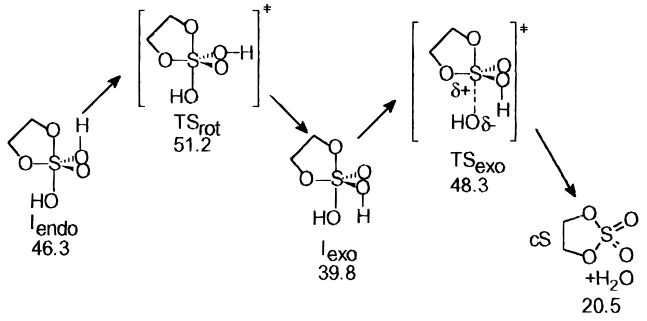

Figure 6. Structures along reaction−energy profile for intramolecular sulfuryl group transfer via pathway NC. See Figure 1d for detailed structures. Annotated numbers are relative energies including zero point energy, kcal/mol (Table 2).

the overall free energy barrier for intramolecular sulfate group migration by pathway NP, via the rate-determining transition state $\mathbf{TS}_{PR}$, is 45.2 kcal/mol (Figure 5).

In TBP sulfuranes, an eclipsing interaction with the equatorial O−H bond serves to increase the apical S−O bond length.[25] This interaction may strongly activate the apical group toward departure and is required for progress along the NC pathway (Figures 1d and 6). Exocyclic cleavage from $\mathbf{I}_{endo}$ predicates rotation about the equatorial S−O bond to place the equatorial hydroxyl hydrogen

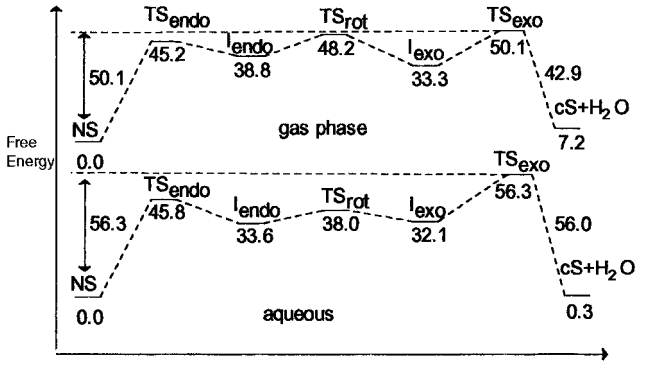

Figure 7. Free energy−reaction profile for pathway NC (see Figures 1 and 6). Annotated numbers are relative Gibbs free energies calculated at the MP2/6-31+G*//HF/3-21G(*) level in the gas phase, kcal/mol. Relative free energies in aqueous solution include a solvation free energy calculated for the gas phase structures (Table 2).

cis to the apical hydroxy ligand in $\mathbf{I}_{exo}$. There is, of course, a rotational transition state associated with this process. This transition state, $\mathbf{TS}_{rot}$, was located with the equatorial O−H bond approximately in the equatorial plane (Figure 1d). The energies calculated for $\mathbf{TS}_{rot}$ and $\mathbf{I}_{exo}$ yield an activation energy for rotation from the endocyclic-eclipsed intermediate $\mathbf{I}_{endo}$ of ~5 kcal/mol (Figure 6, Table 3) with a rotational free energy of activation of 9.4 kcal/mol (Figure 7, Table 3).

Considering the reverse reaction, cleavage of the endocyclic S−O bond of $\mathbf{I}_{endo}$ to give **NS**, departure of the apical ligand was seen to be concerted with proton transfer. The same concerted proton transfer was observed in dissociation of $\mathbf{I}_{exo}$ to give the cyclic sulfate **cS**, with water as the leaving group. The reaction coordinate under examination corresponds to the exocyclic S−O bond length. This S−O bond length is 1.662 Å in $\mathbf{I}_{exo}$ increasing to approximately 2.1 Å at the transition state $\mathbf{TS}_{exo}$. The reaction energy profile shows that the transition state for exocyclic cleavage is 8.5 kcal/mol higher than the preceding intermediate (Figure 6). The free energy of activation for cyclization via pathway NC is calculated as 50.1 kcal/mol (Figure 7). The full reaction scheme for sulfuryl group transfer via pathway NC requires attack of water on **cS** and subsequent cleavage (eq 2; also see Scheme 1, Figure 1d).

$$\mathbf{NS} \rightarrow \mathbf{TS}_{endo} \rightarrow \mathbf{I}_{endo} \rightarrow \mathbf{TS}_{rot} \rightarrow \mathbf{I}_{exo} \rightarrow \mathbf{TS}_{exo} \rightarrow \mathbf{cS} + H_2O \rightarrow \mathbf{TS}_{exo} \rightarrow \mathbf{I}_{exo} \rightarrow \mathbf{TS}_{rot} \rightarrow \mathbf{I}_{endo} \rightarrow \mathbf{TS}_{endo} \rightarrow \mathbf{NS} \quad (2)$$

Solvation. Various solvation models are under development for calculation of solution-phase energy data. Many posit that solvation energies can be added to energies obtained for structures calculated in the gas phase.[28] In this approach, the assumption, usually implicit, is that structures obtained in the gas phase mirror structures along the reaction profile in solution. This assumption is weakest for the dissociative, long-range, gas-phase transition states such as $\mathbf{ATS}_{exo}$ and for reactions of anions, in which aqueous solvation energies are large. However, in order to obtain an approximate measure of reaction profiles in solution and

(28) See references in: Cramer, C. J., Truhlar, D. G., Eds. *ACS Symposium Series*; American Chemical Society: Washington, DC, 1994; Vol. 568.

to provide comparison with related phosphate systems where this approach has been used, the CDM aqueous solvation model of Lim and Chan was employed.[16,17] This CDM model is very similar to the solvation model used by both Karplus' and Lim's groups to obtain solution energy profiles for reactions of phosphates.[17,22] Atomic radii and charges at atoms are required input parameters in the CDM algorithm. Relative aqueous solvation energies calculated using HF/CHELP charges and radii of 1.95, 2.015, 1.75, and 1.5 Å for C, S, O, and H, respectively, differ from those calculated using MP2/Mulliken (MK1) charges by 0.4−9 kcal/mol (Tables 1 and 2). Modifying the radius of the hydroxyl hydrogen to 0.73 Å produced differences in relative solvation energy, calculated with Mulliken charges (MK2), of a similar magnitude. The absolute solvation energies for $\mathbf{AI}_{TBP}$, calculated with these three parameter sets, are −80.01, −80.49, and −84.85 kcal/mol for CHELP, MK1, and MK2 parameters respectively (Table 1). By varying charge type and atomic radii, an aqueous solvation energy of −95 to −110 kcal/mol can be obtained for hydroxide ion, compared with experimental estimates of −89 to −104 kcal/mol.[29,30] Thus a fixed value of −98 kcal/mol was chosen to provide comparison with the work of Lim's group.[17]

Incorporating aqueous solvation energy in calculation of overall free energy in solution yields free-energy profiles for reaction in solution (Figures 3, 5, and 7). The major effects of solvation are (i) to lower the relative energies of ethylene sulfate plus hydroxide (or plus water), and (ii) to lower the energy of pathway AC relative to the alternative CP pathway.

Discussion

Sulfates vs Phosphates. Phosphate and sulfate esters are negatively charged at physiological pH. Furthermore, the parent inorganic anions are almost identical in size. Subtle differences must, of course, exist since many proteins are capable of differentiating these species. For example, bacterial periplasmic binding proteins are found to bind inorganic sulfate over inorganic phosphate (and *vice versa*) by factors of $>10^5$, relying primarily on hydrogen-bonding interactions.[31−33] Comparison of sulfate with phosphate ester reactivity provides a useful frame of reference.

The mechanisms of reaction of phosphate esters are relatively well understood on the basis of thorough analysis by many research groups, and *Westheimer's Guidelines*, in particular, provides a sound mechanistic framework.[6,7,34−37] Dissociative and associative mechanisms of nucleophilic substitution at phosphorus have been discussed, although associative and "preassociative" mechanisms dominate the aqueous solution chemistry of phosphate esters.[6,38] *Westheimer's Guidelines* and related mechanistic analyses support and are founded upon the assumption of trigonal bipyramidal (TBP) pentacoordinate reaction intermediates and transition states in these associative reactions.[39,40] Although only spirocyclic pentacoordinate hydroxyphosphoranes have been isolated,[40] this assumption is supported by a good literature of MO calculations pioneered by Gorenstein.[41] In recent years, such MO calculations have supported and in some cases challenged the dogma of mechanistic phosphorus chemistry.[17−24] However, such calculations are able to demonstrate features of the *Guidelines* including: (a) the isomerization of TBP intermediates following the Berry coordinate for pseudorotation (referred to simply as pseudorotation);[26] (2) the concept of relative apicophilicity, defining the relative propensity of a ligand to occupy the apical rather than equatorial position in a TBP intermediate,[19,24] and (3) the propensity of five-membered rings for apical/equatorial attachment.

Understanding of the reactivity of sulfate esters, despite the work of Kaiser and others, is far less developed.[8,9,42−47] *In simile* with phosphate esters, dissociative processes are not indicated to be important in aqueous solution for sulfates. In contrast to phosphates, nucleophilic attack at C with ensuing C−O bond cleavage is always a highly competitive process and overwhelms nucleophilic substitution at S in aliphatic sulfate diesters. Conversely, sulfate monoesters, the important biological species, are not highly reactive in aqueous solution: the half-life for 2,4-dinitrophenyl sulfate hydrolysis at pH 6.8 and 25 °C is >4 h.[48]

Whereas experimental results require TBP pentacoordinate intermediates in many nucleophilic substitution reactions at phosphorus in phosphate esters, there are no similar observations requiring such intermediates in nucleophilic substitution reactions of sulfate esters.[42] Williams and co-workers have shown in studies performed on highly activated aryl sulfamidate esters that reactions at sulfur may proceed with a highly exploded transition state, similar to S_N2 reaction at carbon.[49,50] Kinetic data has been interpreted to require pentacoordinate intermediates in reactions of aryl sulfonate and sulfonamidate esters.[51−53] We have previously shown that pentacoordinate, TBP, pentaoxysulfurane intermediates, similar to those located in investigations on phosphate esters, may be located using *ab initio* MO calculations in the gas phase for the model systems $H_3SO_5^-$ and $H_2SO_5CH_3^-$.[54,25]

(29) Gomer, R.; Tryson, G. *J. Chem. Phys.* **1977**, *66*, 4413.
(30) Pearson, R. G. *J. Am. Chem. Soc.* **1983**, *108*, 6109.
(31) He, J. J.; Quiocho, F. A. *Science* **1991**, *251*, 1479.
(32) Thatcher, G. R. J.; Cameron, D. R.; Nagelkerke, R.; Schmitke, J. *J. Chem. Soc., Chem. Commun.* **1992**, 386.
(33) Kanyo, Z. F.; Christianson, D. W. *J. Biol. Chem.* **1991**, *266*, 4264.
(34) Ugi, I.; Ramirez, F. *Chem. Br.* **1972**, *8*, 198.
(35) Trippett, S. *Phosphorus Sulfur* **1976**, *1*, 89.
(36) Mislow, K. *Acc. Chem. Res.* **1970**, *3*, 321.
(37) Muetterties, E. L.; Mahler, W.; Schmutzler, R. *Inorg. Chem.* **1963**, *2*, 613.
(38) Jencks, W. P.; Herschlag, D. *J. Am. Chem. Soc.* **1989**, *111*, 7579.
(39) Holmes, R. R. *Pentacoordinated Phosphorus*; American Chemical Society: Washington DC, 1980; Vols. 1 and 2.
(40) For example: Dubourg, A.; Roques, R.; Germain, G.; DeClercq, J.-P.; Garrigues, B.; Boyer, D.; Munoz, A.; Klaebe, A.; Comtat, M. *J. Chem. Res. (S)* **1982**, 180.
(41) Gorenstein, D. G.; Luxon, B. A.; Goldfield, E. M. *J. Am. Chem. Soc.* **1980**, *102*, 1759.
(42) Kaiser, E. T. *Acc. Chem. Res.* **1970**, *3*, 145.
(43) Kaiser, E. T.; Panar, M.; Westheimer, F. H. *J. Am. Chem. Soc.* **1963**, *85*, 602.
(44) Benkovic, S. J.; Benkovic, P. A. *J. Am. Chem. Soc.* **1966**, *88*, 5504.
(45) Kice, J. L. *Adv. Phys. Org. Chem.* **1980**, *17*, 65.
(46) Laleh, A.; Ranson, R.; Tillett, J. G. *J. Chem. Soc., Perkin Trans. 2* **1980**, 610.
(47) Mikolajczyk, M. *Phosphorus Sulfur* **1986**, *27*, 31.
(48) Davis, J. M.; Cameron, D. R.; Kubanek, J. M.; Mizuyabu, L.; Thatcher, G. R. J. *Tetrahedron Lett.* **1992**, 2205.
(49) Bourne, N.; Hopkins, A.; Williams, A. *J. Am. Chem. Soc.* **1985**, *107*, 4327.
(50) D'Rozario, P.; Smyth, R. L.; Williams, A. *J. Am. Chem. Soc.* **1984**, *106*, 5027.
(51) Graafland, T.; Wagenaar, A.; Kirby, A. J.; Engberts, J. B. F. N. *J. Am. Chem. Soc.* **1979**, *101*, 6981.
(52) Wagenaar, A.; Engberts, J. B. F. N. *J. Org. Chem.* **1988**, *49*, 3445.
(53) Suh, J.; Kim, J.; Lee, C. S. *J. Org. Chem.* **1991**, *56*, 4364.

Studies on isolable phosphoranes, in particular by Trippett and Holmes, have aided study on phosphate reactions.[35,39] Likewise, Martin and co-workers have synthesized various hypervalent sulfurane species suggesting that TBP sulfuranes are feasible intermediates in reactions at sulfur, although *in simile* with phosphorus chemistry, pentacoordinate reaction intermediates themselves are not observable on the NMR time scale.[55−57] However, it has often been stated that pseudorotational processes should be less likely and less facile for sulfuranes than phosphoranes.[42,46,58,59] The rationales for this assertion are based largely upon: (1) X-ray structure determinations showing that sulfuranes are less likely to distort from TBP to SP structures (the structure of the transition state for Berry pseudorotation is SP; and (2) the stereochemistry of nucleophilic substitution at sulfur.[60]

Hypothetical Intramolecular Group Transfer Mechanisms. Acetate and phosphate groups of *vic*-diols are known to migrate to adjacent hydroxyl groups in aqueous solution under relatively mild conditions.[61−65] Migrations of phosphates in biological systems have been observed[66,67] and work-up conditions can also lead to intramolecular phosphate group migration in synthesis and separation procedures.[68] In contrast, alkyl sulfates appear quite stable toward migration. Despite the extensive literature on sugar sulfate synthesis, to the best of our knowledge there are no published examples of facile intramolecular sulfate group transfer.[69,70] Three main reasons exist for directing attention toward intramolecular transfer. First, the stability of sulfate groups toward migration may be associated with the choice of sulfates as regiospecific molecular recognition units on GAG sulfates. Second, the excellent experimental and computational data on the analogous phosphoryl transfer processes allows comparison with data for sulfuryl transfer. Finally, intramolecular reactions and neighboring group participation provide model systems for enzymes, frequently exploited by experimentalists.[71]

Scheme 3

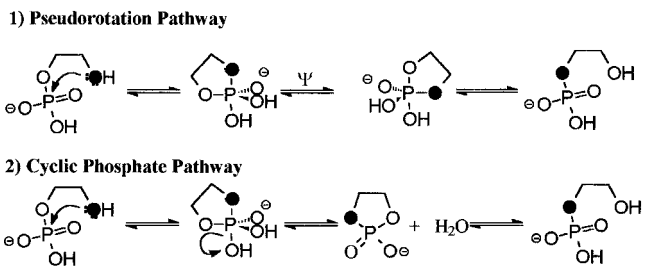

When *Westheimer's Guidelines* is applied, two associative mechanisms for intramolecular phosphoryl transfer are possible (Scheme 3): (1) In-line attack of the 2-OH nucleophile on phosphorus to form an initial TBP intermediate, proton transfer, and subsequent pseudorotation to a final TBP intermediate, followed by expulsion of the apical leaving group; and (2) in-line attack and loss of water to form a cyclic tetracoordinate intermediate, followed by hydrolytic ring cleavage to yield a mixture of 1- and 2-phosphate products. An important concept of the *Guidelines* is the apical ingress and egress, of nucleophile and leaving group respectively, in the TBP intermediate. Owing to the arrangement of incoming and leaving groups in the initial TBP intermediate the first pathway is described as an *adjacent* mechanism and the second *in-line*.[6,7]

Intramolecular 1,2-phosphate group transfer was explored in the classic chiral phosphate experiment of Knowles and co-workers using stereochemical analysis of reaction at P as the experimental tool. Both pseudorotation and cyclic phosphate pathways (Scheme 3) are competitive in acidic aqueous solution. The mechanism of formation and reaction of five-membered cycilc phosphates has also been studied extensively by MO calculations, owing to the obvious relevance to RNA chemistry and the mechanism of ribonuclease. In the gas phase, activation barriers to pseudorotation have been calculated at $\Delta G^{\neq} = 2$ kcal/mol[26a] and $\Delta G^{\neq} = 12$ kcal/mol.[23] Applying *Westheimer's Guidelines* to intramolecular sulfuryl group transfer in 2-hydroxyethyl sulfate yields two anionic pathways for neutral solution (Scheme 1) and two neutral pathways for acidic solution (Scheme 2), comparable to those for phosphates (Scheme 3).

Calculated Reaction Pathways in Neutral Solution. In-line attack of the 2-OH to form a TBP intermediate places an oxyanion ligand at the apical position of the initial TBP structure ($\pm\mathbf{I}_{TBP}$, Scheme 1). This is a disallowed process for phosphates and also for sulfates. Placement of an anionic oxygen at the apical position of a TBP which possesses greater electron density than the equatorial positions is highly energetically unfavorable and no such pentacoordinate structures can be located.[25] An alternative route involves proton transfer prior to cyclization (Scheme 1). In path AP, the initial TBP intermediate must pseudorotate to put the leaving group in the apical position in a second TBP intermediate. This again places an oxyanion at the apical position of a TBP ($\mathbf{AI}_{ap}$) and thus this pseudorotation is predicted to be disallowed. The alternative "allowed" pathway AC proceeds via a five-membered sulfate intermediate (Scheme 1). Interestingly, the "disallowed" pseudorotation is avoided, but motion along the pseudorotation coordinate promotes S−O bond cleavage. Indeed, the structures shown in Figure 2 provide four routes for intramolecular sulfate group migration. The simplest, pathway AC, proceeds via cyclic sulfate, **cS** (Figure 1b). The second,

(54) MO calculations previously performed on pentacoordinate TBP structures related to the experimental sulfonamidate system (refs 51 and 52) included significant geometry constraints (no full geometry optimization was performed on any of the intermediates or "transition states" explored), see: Graafland, T.; Nieuwpoort, W. C.; Engberts, J. B. F. N. *J. Am. Chem. Soc.* **1981**, *103*, 4490.

(55) Perkins, C. W.; Wilson, S. R.; Martin, J. C. *J. Am. Chem. Soc.* **1985**, *107*, 3209.

(56) Hayes, R. A.; Martin, J. C. *Stud. Org. Chem.* **1985**, *19*, 408.

(57) Astrologer, G. W.; Martin, J. C. *J. Am. Chem. Soc.* **1976**, *98*, 2875.

(58) Holmes, R. R. *Acc. Chem. Res.* **1979**, *12*, 257.

(59) Tang, R.; Mislow, K. *J. Am. Chem. Soc.* **1969**, *91*, 5644.

(60) Many of the sulfuranes studied possess one or more pair of nonbonding electrons on sulfur which may significantly alter structure and dynamics relative to pentaoxysulfuranes.

(61) Buchwald, S. L.; Pliura, D. H.; Knowles, J. R. *J. Am. Chem. Soc.* **1984**, *106*, 4917.

(62) Fordham, W. D.; Wang, J. H. *J. Am. Chem. Soc.* **1967**, *89*, 4197.

(63) Brown, D. M.; Magrath, D. I.; Neilson, A. H.; Todd, A. R. *Nature* **1956**, *177*, 1124. Kilgour, G. L.; Ballou, C. E. *J. Am. Chem. Soc.* **1959**, *81*, 915. Anderson, L.; Landel, A. M. *J. Am. Chem. Soc.* **1954**, *76*, 6130.

(64) Oivanen, M.; Schnell, R.; Pfleiderer, W.; Lonnberg, H. *J. Org. Chem.* **1991**, *56*, 3623.

(65) Reese, C. B.; Skone, P. A. *Nucl. Acids Res.* **1985**, *13*, 2451.

(66) Posternak, T. *Helv. Chim. Acta* **1958**, *41*, 1891.

(67) Breslow, R.; Huang, D. *J. Am. Chem. Soc.* **1990**, *112*, 9621.

(68) Norman, D. G.; Reese, C. B.; Serafinowska, H. T. *Tetrahedron Lett.* **1984**, 3015.

(69) See references in: Schweiger, R. G., Ed. *ACS Symposium Series*; American Chemical Society: Washington, DC, 1978; Vol. 77.

(70) Some experimental evidence exists for intramolecular transfer via reaction at other sulfur centres, see: Andersen, K. K.; Chumpradit, S.; McIntyre, D. J. *J. Org. Chem.* **1988**, *53*, 4667. White, E. H.; Lim, H. M. *J. Org. Chem.* **1987**, *52*, 2162.

(71) Kirby, A. J. *Adv. Phys. Org. Chem.* **1980**, *17*, 183.

pathway CP, proceeds from the tautomer **BS** with apical attack of nucleophile, but equatorial departure of the leaving group from the initially formed TBP intermediate, $\mathbf{AI}_{TBP}$ (Figure 1a). Since equatorial S−O bond cleavage from $\mathbf{AI}_{TBP}$ yields the acyclic sulfate, **AS**, directly, the reverse reaction provides a third and fourth route for intramolecular migration: cyclization of **AS** via equatorial nucleophilic attack, followed by apical departure of leaving group, either to form **cS** or alternatively to give **BS**. The energy barriers for these last two routes are clearly identical to those for pathways AC and PC respectively (Figures 1a, 2, and 3).

In pathway AC, via cyclic sulfate, the high energy of hydroxide ion in the gas phase causes destabilization of **cS** + OH^- and the preceding transition state, $\mathbf{ATS}_{exo}$, which is itself very close in energy and structure to dissociated **cS** plus hydroxide (Figures 1b and 3). In the gas phase, the free energy of activation is calculated as 86 kcal/mol for intramolecular sulfate transfer via pathway AC. Aqueous solvation profoundly stabilizes hydroxide, lowering the relative energies of $\mathbf{ATS}_{exo}$ and the dissociation products (Figure 3). The barrier to sulfate migration is substantially reduced: $\Delta G^{\neq}$ (aq) = 59 kcal/mol.

In pathway CP, the effects of aqueous solvation are moderated, but because of the fine balance of the energies of the three pentacoordinate structures along the reaction profile, solvation does cause a change in rate-determining step (Figure 3). In the gas phase, $\Delta G^{\neq}$ = 63 kcal/mol, the rate-determining step being formation of the TBP intermediate, $\mathbf{BS} \rightarrow \mathbf{AI}_{TBP}$. However, in aqueous solution the activation barrier is calculated to drop to 52 kcal/mol and the rate-determining step becomes breakdown of the TBP intermediate, $\mathbf{AI}_{TBP} \rightarrow \mathbf{AS}$. Regardless, the barriers to sulfate group migration by either of the four possible routes are substantial in both the gas phase and aqueous solution. Furthermore, given the possible errors in the solvation model, it is reasonable to estimate that reactions via bond forming/breaking of the equatorial and the apical S−O bonds of the TBP intermediate might be nearly isoenergetic.

Calculated Reaction Pathways in Acidic Solution. On the basis of the *Guidelines*, problems with "disallowed" intermediates and pseudorotation are not envisaged in cyclization of the neutral hydroxyethyl sulfate (Scheme 2). Indeed, cyclization and pseudorotation proceed in a comparable fashion to the analogous phosphates (Figures 1c and 3). The gas-phase reaction profile for sulfate migration via the pseudorotational pathway (NP; Scheme 2, Figure 1c) is characterized by an energy plateau of five pentacoordinate structures within 6 kcal/mol of each other (Figure 5). The free energy barrier for pseudorotation via the anticipated square pyramidal transition state is calculated to be 3 kcal/mol or less in the gas phase and solution. Pseudorotation does not represent a rate-limiting step. In the gas phase and aqueous solution, cyclization is rate determining and the calculated $\Delta G^{\neq}$ = 45−46 kcal/mol.

Migration via pathway NC and cyclic sulfate formation requires exocyclic cleavage from the originally formed TBP intermediate, $\mathbf{I}_{endo}$ (Figures 1d and 6). *In simile* with calculations on phosphoranes, rotation about the equatorial S−O(H) bond is required for exocyclic cleavage.[17,18,21−23,41] Previous calculations on sulfuranes have indicated that the synperiplanar interaction of an equatorial O−H bond with an apical ligand is stabilizing, owing to internal hydrogen bonding.[25] Similarly, the

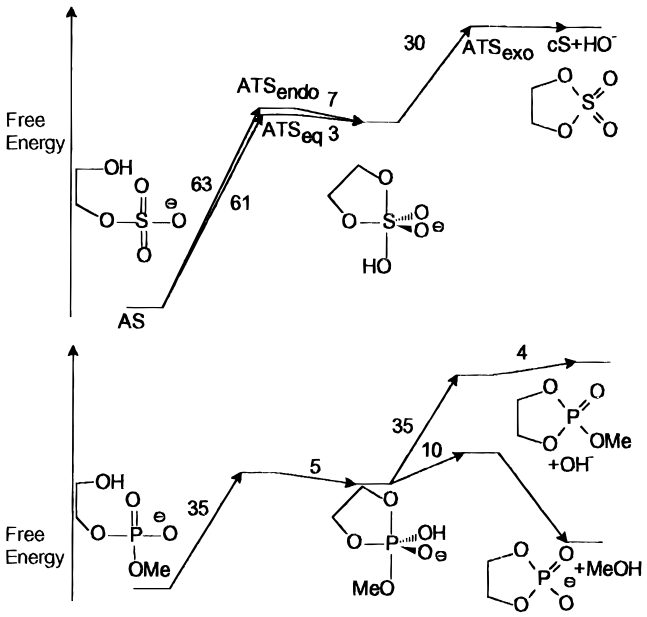

Figure 8. Simplified free energy−reaction profile for sulfate cyclization via pathways CP and AC calculated in the gas phase (Figure 3, Table 1), compared to free energy−reaction profile for similar phosphate cyclization from ref 17 [MP2/6-31+G*//HF/3-21+G(*)]. Several intermediates and transition states are not shown in order to increase clarity. Calculated values of ΔG (kcal/mol) are shown for each step.

synperiplanar interaction of the equatorial O−H with the nucleophile and nucleofuge in the pentacoordinate transition states, $\mathbf{TS}_{endo}$ and $\mathbf{TS}_{exo}$, is stabilizing because of internal hydrogen bonds. Indeed, the hydrogen bond in $\mathbf{TS}_{exo}$ leads to expulsion of water rather than hydroxide. The energy barrier for rotation about the equatorial S−O bond is suprisingly large relative to the related pseudorotational process: $\Delta G^{\neq}_{rot}$ = 10−15 kcal/mol (Figures 5 and 7). However, the rate-determining step calculated in both the gas phase and aqueous solution is exocyclic cleavage from the second TBP intermediate $\mathbf{I}_{exo}$. In contrast to the anionic exocyclic cleavage transition state, $\mathbf{ATS}_{exo}$, the neutral equivalent, $\mathbf{TS}_{exo}$, is compact and internally hydrogen bonded, thus aqueous solvation is not calculated to lower the reaction barrier via this transition state. The reaction barrier in solution is actually calculated as higher than that in the gas phase, $\Delta G^{\neq}$ = 50 kcal/mol, $\Delta G^{\neq}$(aq) = 56 kcal/mol (Figure 7). Thus pathway NC is less favorable than the pseudorotational pathway (NP) by 10 kcal/mol in solution. Nevertheless, the barrier to sulfate group migration in solution, $\Delta G^{\neq}$ = 46 kcal/mol, appears significant.

Comparison with Phosphate Reactivity. Previous MO calculations, directed at reaction at phosphorus and the resulting pentacoordinate phosphorane intermediates and transition states, provide an invaluable basis for comparison of the present data, in particular since similar solvation models and levels of calculation have been employed.[17,18,20,22] Data for cyclization of hydroxyethyl sulfate anion may be compared with the data of Lim and Tole for cyclization of methyl hydroxyethyl phosphate (MHEP) (Figure 8).[17] In the gas phase, cyclization of the sulfate to form a TBP intermediate is almost twice as costly energetically as cyclization of the phosphate. The rationale most reasonably rests on the requirement for reaction of the sulfate via either the highly unfavorable tautomerism of **AS** ($\Delta G^{\neq}$ = 63 kcal/mol), or cyclization via equatorial attack ($\Delta G^{\neq}$ = 61 kcal/

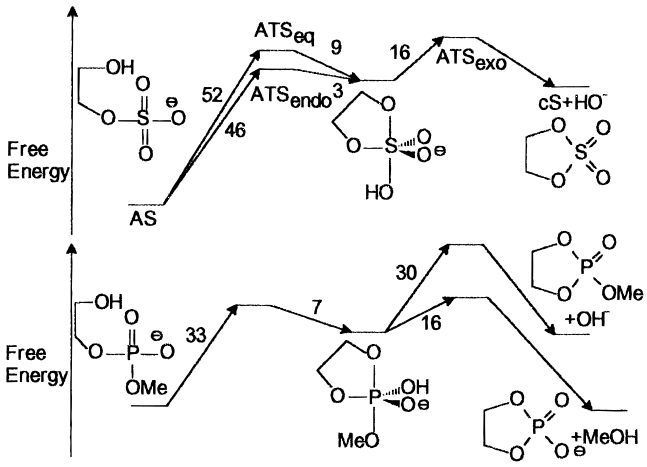

Figure 9. Simplified free energy-reaction profile for sulfate cyclization via pathways CP and AC calculated with aqueous solvation corrections applied (Figure 3, Table 1), compared to free energy−reaction profile for similar phosphate cyclization from ref 17 [MP2/6-31+G*//HF/3-21+G(*)]. Several intermediates and transition states are not shown in order to increase clarity. Calculated values of ΔG (kcal/mol) are shown for each step. A similar solvation model was employed by Tole and Lim.

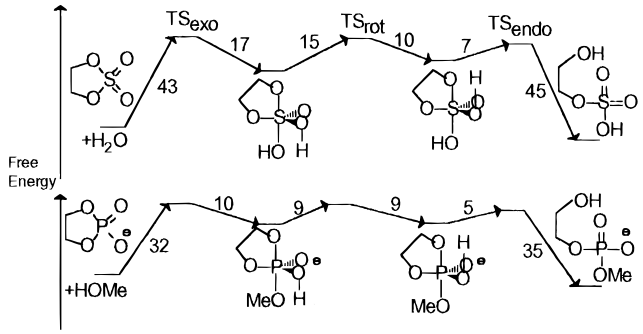

Figure 10. Simplified free energy−reaction profile for hypothetical sulfate ring-opening via pathway NC calculated in the gas phase (Figure 7, Table 2), compared to free energy−reaction profile for similar phosphate ring cleavage derived from ref 17 [MP2/6-31+G*//HF/3-21+G(*)]. Several intermediates and transition states are not shown in order to increase clarity. Calculated values of ΔG (kcal/mol) are shown for each step.

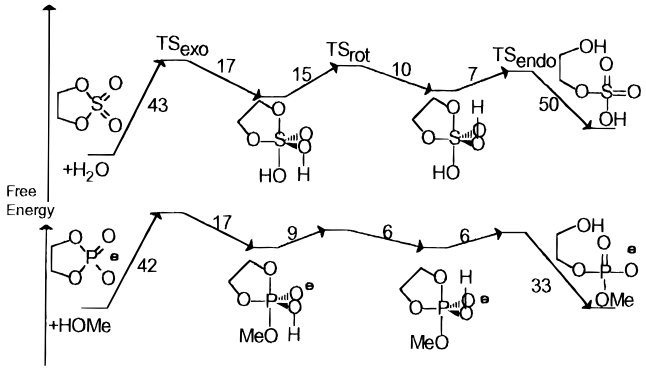

Figure 11. Simplified free energy−reaction profile for hypothetical sulfate ring opening via pathway NC calculated with aqueous solvation corrections applied (Figure 7, Table 2), compared to free energy−reaction profile for similar phosphate ring cleavage derived from ref 17 [MP2/6-31+G*//HF/3-21+G(*)]. Several intermediates and transition states are not shown in order to increase clarity. Calculated values of ΔG (kcal/mol) are shown for each step. A similar solvation model was employed by Tole and Lim.

mol) (Figure 8). Indeed, expulsion of hydroxide from the TBP intermediate is slightly more favorable for the sulfurane than phosphorane.

Calculated energy profiles for reaction in solution show a similarly high barrier for formation of the TBP intermediate for sulfate relative to phosphate.[17] The transition states for exocyclic cleavage from the TBP intermediate for reaction of the phosphate are similar to $\mathbf{ATS}_{eq}$ and $\mathbf{TS}_{exo}$ in that internal hydrogen bonding minimizes the stabilization by solvation. Thus, $\mathbf{ATS}_{exo}$ which has no such internal hydrogen bonding is more profoundly stabilized by solvation than its phosphate counterparts (Figure 9). These calculations indicate the free energy of activation for cyclization in aqueous solution to be of a similar high magnitude for formation of methyl ethylene phosphate and ethylene sulfate. There is, of course, no evidence for cyclization of *vic*-diol monosulfates in the pH region under question,[72] nor reaction of MHEP to give methyl ethylene phosphate. Conversely, pH-independent phosphate group migration of the methyl esters of 2′- and 3′-AMP proceeds via a putative cyclic TBP intermedaite with $\Delta G^{\neq} = 31$ kcal/mol at 363 K and is at least a factor of 10 more rapid than expulsion of methanol (cf. Figure 9).[64]

The reverse reaction of methyl hydroxyethyl phosphate cyclization is methanolysis of ethylene phosphate. This hypothetical reaction may be compared to pH-independent hydrolysis of ethylene sulfate (Figures 10 and 11). In the gas phase, the dynamics of the two processes are identical and the reaction−energy profiles bear some similarity (Figure 10). Nucleophilic attack on the cyclic reactants is rate determining with $\Delta G^{\neq} = 32-43$ kcal/mol. The phosphate reactant carries a formal negative charge. The simple electrostatic argument would predict that the energy barrier for nucleophilic attack on an anion should be larger; however, calculations indicate the opposite. In fact, summed Mulliken charges on the four oxygens of ethylene sulfate and ethylene phosphate are similar: −3.0 and −2.8 respectively, at the HF/3-21+G(*) level. It is clear from calculations on phosphoranes that a methoxy group has a greater ability than hydroxy to accommodate the high electron density at the apical position of a TBP, thus stabilizing a pentacoordinate intermediate. However, consideration of Figures 8 and 10 suggests that the pentacoordinate state may be intrinsically destabilized relative to the tetracoordinate state for sulfates compared to phosphates. That is the energy required to achieve a pentacoordinate structure on nucleophilic addition is intrinsically greater for sulfates than for phosphates.[73]

The effect of aqueous solvation on the reaction profiles is similar for both systems, despite the difference in charge state (Figure 11). Free energy barriers of 42−56 kcal/mol are indicated, in some accord with experimental

(72) Brimacombe, J. S.; Foster, A. B.; Hancock, E. B.; Overend, W. G.; Stacey, M. *J. Chem. Soc.* **1960**, 201.

(73) This conclusion is based upon the comparison of phosphate and sulfate free energy−reaction profiles and applies to neutral and anionic sulfates and sulfuranes. However, the structure of most neutral sulfur species was obtained at the HF/3-21G(*) level. Therefore, the energies of **NS** and $\mathbf{I}_{endo}$ were compared at higher levels to check the validity of conclusions at the lower level of calculation. At MP2/6-311+G**//HF/6-311G*, the sulfurane is −51.9 kcal/mol above the sulfate reactant, confirming the high relative energy of the pentacoordinate sulfur species.

observations: ethylene sulfate is reactive toward hydrolysis, but as an alkylating agent[74] and cyclic phosphate diesters are relatively stable in neutral aqueous solution.[75]

***Westheimer's Guidelines* and Nucleophilic Substitution at Sulfur.** There is little experimental evidence to support the application of *Westheimer's Guidelines* to reactions at sulfur, in particular, since there is no imperative for invoking pentacoordinate intermediates for reactions of sulfate esters. The present calculations clearly support the extension of the *Guidelines* to nucleophilic substitution at sulfur.

1. Pentacoordinate intermediates and transition states control the associative reactions of sulfate esters.

2. The pentacoordinate intermediates are distorted trigonal bipyramidal.

3. A five-membered ring is attached apical−equatorial in these TBP intermediates.

4. An electron-rich oxyanion is sufficiently poorly apicophilic that it will not be found at the apical position of a TBP.

5. Isomerization of TBP intermediates, via Berry pseudorotation and a pentacoordinate, SP transition state, is energetically facile.

The similar low-energy barriers to pseudorotation calculated for sulfuranes and phosphoranes are at odds with the proposal, on the basis of experiment, that significantly greater barriers would exist for sulfuranes. However, there are substantial structural differences between the sulfuranes studied experimentally and the reaction intermediates studied herein.[60]

The present calculations show that the dynamics of reactions of phosphate and sulfate esters are very similar. The requirement for a synperiplanar relationship between an equatorial substituent (i.e. S−O−H, P−O−Me) and the scissile apical bond, previously noted for TBP phosphoranes, is also observed in sulfurane intermediates.[17,18,21,22] This is a result of the strength of intramolecular electrostatic interactions in the gas phase (*vide supra*).[19,23,25] Furthermore, equatorial entry/departure, a violation of *Westheimer's Guidelines*, is also partly a consequence of strong intramolecular electrostatic interactions in the gas phase. Breakdown of TBP intermediate $\mathbf{AI}_{TBP}$ proceeds via the transition state, $\mathbf{ATS}_{eq}$, with cleavage of the equatorial S−O bond, contrary to the apical entry/departure rule (Figure 1a). The surprising ease of cleavage of the equatorial bond results from two factors: (i) an intramolecular H bond between the departing oxygen and the apical hydroxy hydrogen; and (ii) the initial reaction coordinate being identical to the energetically accessible Berry pseudorotation coordinate (*vide supra*). Previous calculations have indicated reaction pathways involving equatorial entry/departure in the TBP intermediates in reactions of phosphates and phosphoramidates.[20,23,76] This breakdown of the *Guidelines* would be of serious consequence for analysis of reaction stereochemistry if the gas phase results are found to be transferable to solution. The concept of apical entry and departure requires in-line substitution and adjacent substitution with pseudorotation to occur with inversion and retention of stereochemistry respectively (Scheme 3).

Scheme 4

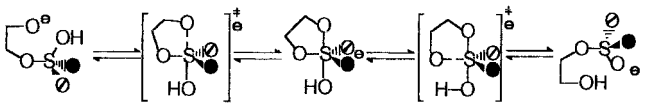

These precepts underlie the chiral phosphate experiment that has been used to great effect in analysis of the stereochemistry of enzyme reactions, where retention of stereochemistry is taken to indicate reaction via two in-line substitutions.[77] No experimental data exists to confirm nor debunk equatorial entry/departure leading to retention of stereochemistry without pseudorotation.

Implications for Nucleophilic Substitution at Sulfur. Why is intramolecular sulfate group migration not observed experimentally? The hypothetical mechanisms proposed in Schemes 1 and 2 provided two possible answers. First, in order to form a TBP intermediate, the sulfate group must be protonated: proton transfer from alcohol to sulfate (Scheme 1) is thermodynamically highly unfavorable; and the pK_a for sulfate monoester protonation (Scheme 2) is very low. Second, doubt has been cast on the viability of pseudorotational processes in cyclic sulfuranes.[42,46,58−60] Either factor could result in the barrier to the competitive reaction, S_N2 reaction at carbon, being more favorable for reaction of sulfates. The calculations presented herein demonstrate high barriers to intramolecular group transfer in both ionized and nonionized *vic*-diol monosulfates. However, the barrier to pseudorotation is shown to be low and comparable to that for phosphate. Free energy−reaction profiles for reaction of the ionized sulfate ester show that the alkoxide tautomer **BS** is substantially more reactive, but confirm the high energy cost associated with proton transfer (Figure 3). Although the sulfate monoanion, **AS**, may cyclize directly (via $\mathbf{ATS}_{eq}$), there is no saving in energy. However, comparison with reaction-energy profiles for nucleophilic substitution at phosphorus suggests that the pentacoordinate state may be of relatively higher energy in reactions at sulfur (Figures 8−11). Thus (1) the ionized sulfate ester **AS** is of low reactivity because of the requirement for proton transfer before or during cyclization, and (2) the nonionized reactant, **NS**, is poorly reactive because of the high intrinsic energy of the pentacoordinate sulfurane reaction intermediates.

Sulfuryl group transfer is catalyzed *in vivo* by sulfotransferase enzymes and sulfurylation is an important biological process, in particular in synthesis of the GAG sulfates.[1,3] Given the high intrinsic energy of the pentacoordinate state, if an associative mechanism is to be followed, catalysis by stabilization of the pentacoordinate state is likely to be even more important than in phosphoryl transfer. Intramolecular reactions are often described as models for enzyme catalyzed reactions.[71] The only sulfuryl transfer process indicated by the present calculations to have an accessible energy barrier is the reaction of **BS** ($\Delta G^{\neq}$(aq) = 23 kcal/mol, Scheme 4). The reaction of an alkoxide nucleophile with the nonionized sulfate group ($-SO_3H$) requires a combination of acid and base catalysis to bring about, but the calculations show that the energy barrier to sulfuryl transfer could be reduced substantially by utilizing such a mechanism (Figure 3; $\Delta G^{\neq}$ = 3 kcal/mol, $\Delta G^{\neq}$(aq) = 23 kcal/mol). Stabilization of the pentacoordinate intermediate, $\mathbf{AI}_{TBP}$ would further lower the barrier. However, it is somewhat

(74) Lohray, B. B. *Synthesis* **1992**, 1035.
(75) Kumamoto, J.; Cox, J. R.; Westheimer, F. H. *J. Am. Chem. Soc.* **1956**, *78*, 4858.
(76) Equatorial entry/departure is feasible in reactions at Si centers and has been proposed for reactions at P, upon this basis, see: Corriu, R. J. P.; Fernandez, J. M.; Guerin, C. *Nouv. J. Chim.* **1984**, *8*, 279.
(77) Knowles, J. R. *Annu. Rev. Biochem.* **1980**, *49*, 877.

disturbing that the stereochemistry of this direct, single displacement reaction is retention at sulfur, since in Lowe's elegant chiral sulfate experiments, retention of stereochemistry is taken as definitive for a double displacement reaction involving a covalent-enzyme intermediate.[78] The only nonenzymic process reported, to date, is sulfate transfer from phenyl sulfate to an alcohol in dry CCl_4 at 100 °C, giving inversion of stereochemistry.[78]

Conclusions

MO calculations suggest that the dynamics of associative nucleophilic substitution at sulfur bear strong similarity to the analogous reaction at phosphorus. Distorted trigonal bipyramidal pentacoordinate intermediates are located and isomerization via Berry pseudorotation does not present a significant energy barrier. *Westheimer's Guidelines* for reaction at phosphorus centers may be extended from reactions of phosphates to those of sulfates. However, equatorial entry of nucleophile and departure of leaving group in the TBP intermediate is indicated to be competitive with apical entry/departure contrary to the *Guidelines*. The absence of observations of intramolecular sulfate migration is compatible with the high calculated energy barriers which result from both a requirement for protonation of the $-SO_3^-$ moiety and the relatively high energy of the pentacoordinate compared to the tetracoordinate state. Cyclization via attack of alkoxide on the nonionized sulfate group ($-SO_3H$) has a calculated free energy of activation in aqueous solution of only 23 kcal/mol, but substantial acid/base catalysis would be required to bring about such reaction. Further MO calculations directed at dissociative mechanisms of sulfuryl group transfer are warranted. In addition experiments to test the possibility of equatorial entry/departure in both sulfate esters and the related phosphate esters are indicated.

Acknowledgment. The author thanks the Natural Sciences and Engineering Research Council Canada and the Petroleum Research Fund administered by the ACS for financial support. Dr. Carmay Lim's provision of the CDM programme is gratefully acknowledged.

JO9521460

(78) Chai, C. L. L.; Loughlin, W. A.; Lowe, G. *Biochem. J.* **1992**, *287*, 805.